AJAB

Asian J Agri & Biol. 2018;6(2):189-197.

Original Research Article

Comparative analysis of some winter crops area estimation using landsat-8 and sentinal-2 satellite imagery

Abdelraouf M. Ali,* Mohamed A. Aboelghar, Mohamed A. El-shirbeny, Nasser H. Salem
National Authority for Remote sensing and space science (NARSS), Cairo, Egypt

Received:
December 31, 2017
Accepted:
May 01, 2018
Published:
June 30, 2018

**Corresponding author email:*
raouf.shoker@narss.sci.eg

Abstract

Estimating crop area is a key factor for any crop monitoring and agricultural management system. Having annual information on crop acreage and production change is sufficient for agricultural decision makers and planners. The aim of this study is to monitor changes in cultivated areas and to estimate wheat crop area using satellite imagery with different spatial resolutions and time series normalize different vegetation index ($NDVI_{Ts}$). The study is focusing on using accuracy assessment from maximum likelihood classification methods applied to multi-spatial resolution scenes (30, 20 and 10 meters) derived from Landsat8 and Sentinel-2 satellites. More specifically, $NDVI_{Ts}$ estimates from Landsat 30m, Sentinel-2 (20m), and (10m) spatial resolutions are compared to discriminate wheat crop. The study area is located in El-Minya governorate, Egypt. The results showed that the accuracy of using $NDVI_{Ts}$ data from different imageries showed higher accuracy than using one single date. The $NDVI_{Ts}$ estimate from the Sentinel-2(10m) has (81%) as an overall accuracy and (0.74) as Kappa coefficient where Sentinel-2(20m) $NDVI_{Ts}$ data has (69.38%) as an overall accuracy and (0.58) as Kappa coefficient. The lowest accuracy (64.38%) and Kappa coefficient (0.51) resulted from occurred with Landsta8 ($NDVI_{Ts}$) data.

Keywords: Crop Area Estimation, NDVI time serious, Landsat-8, Sentinel-2

Introduction

As Egypt is a developing country, high percent of Egyptian population living under the poverty line. Food security is a challenge for the governments and decision makers. Wheat is the most important cereal crop in Egypt. It represents almost ten percent of the national agricultural production and about twenty percent of all imports. Thus, it is logical that wheat is a product of huge importance to the Egyptian society and wheat policy is a priority for any government (FAO, 2015). Timely and costly effective statistics regarding wheat yield is critical for food security and sustainable agricultural development. These statistics enable the governmental agencies and crop producers to manage the wheat production process that includes planning the harvest, the storage, import and marketing activities.

In countries with well-organized agricultural system, post harvest estimates are still the common method. It depends on using ground-based data collection which is costly, time-consuming and labor-intensive. Having reliable statistics attached with a spatial distribution of crop area month/s before harvest is a major challenge in the area of remote sensing agricultural applications. Crop-yield prediction using remotely sensed data recently represents a wide field of research and application (Salazar et al., 2007; Parasad et al., 2006; Manjunath et al., 2002). Satellite remote sensing technology is now providing accurate statistical and

spatial information for yield and production forecast. However, crop classification as an essential step for yield monitoring and mapping is still problematic. Traditional methods such as area sampling, list sampling, point sampling with or without a grid have proven to be successful (Pickup et al., 1993). However, a continuous research is necessary to establish more accurate methods. It is essential for the proposed method to be applicable under local agricultural conditions that might be different from a country to another and sometimes are different even within the same country.
Moderate to high spatial resolution images were used frequently for crop monitoring and to identify cropland areas (Epiphanio et al., 2010). Linear mixture model (LMM) was applied to time series of moderate spatial resolution for vegetation cover identification (Silva et al., 2010). The Moderate Resolution Imaging Spectro-radiometer (MODIS) with 250 m spatial resolution was adequate for identifying large crop fields (Ren et al., 2008; Wardlow et al., 2006). In Egypt, developing a remotely sensed based system for crop mapping is a big challenge because of the highly intensive cultivated lands and the diversity of agricultural production systems, ranging from traditional small farms to high mechanized commodity crop production operations. Therefore, processing of multi temporal and higher spatial resolution satellite imagery is an issue of high necessity.
Sentinel-2 (S2) is characterized by wide-swath, high resolution, multispectral imager with (13) spectral bands. These features offer a unique perspective on land and vegetation (Drusch, 2012). High spatial resolution (up to 10 m), high spectral resolution (three bands in the red-edge and two bands in the SWIR) in combination with a wide coverage and five days revisit time provides applicable data for a wide range of land applications (Malenovský, 2012). The objective of the current study is to investigate changes in cultivated areas using remote sensing satellite imagery with different spatial resolutions and time series normalize different vegetation index ($NDVI_{Ts}$) for estimating wheat crop area.

Material and Methods

Study area

El-Minya governorate is one of the most highly populated governorates of Upper Egypt. It contains 9 cities; 3,375 villages; and 10,875 hamlets. The nine cities from north to south are: Abu Qirqas, El Idwa, Minya, Beni Mazar, Dayr Mawas, Maghaghah, Mallawi, Matay and Samalut as shown in figure (1). Al-Minya has a desert climate. There is virtually no rainfall during the year. The Köppen-Geiger climate classification is BWh. The average annual temperature is 21.3 °C. The average annual rainfall is 1 mm. Most precipitation falls in February with an average of 1 mm. July is the warmest month of the year with an average temperature of (28.2°C). The lowest average temperature of the year is in January with (12.2°C). The difference in precipitation between the driest month and the wettest month is 1 mm and the average temperatures vary by (16.0°C).

Satellite dataset

Six Landsat-8 imageries (Path 177 Row 40 and Path 176 Row 41), with (30) spatial resolution, five Sentinel-2 images with (20 m) and four sentinel-2 (10 m) spatial resolution covering the winter season of (2015 - 2016) were used to produce the detailed crop map. Detailed description of the spectral bands and spatial resolution is shown in table (1) while types of the sensor, acquisition dates are shown in table (2).

Data processing

The Atmospheric correction was carried out using (FLAASH - ENVI) module for two sensors (Landsat-8 and senstinel-2. This module depends on standard equation for spectral radiance at a sensor pixel, L. The equation of this module is as follows in equation No (1) according to (Kaufman et.,al., 1997):

$$L = \left(\frac{A\rho}{1-\rho e\ S}\right) + \left(\frac{B\rho e}{1-\rho es}\right) + La$$

where:

ρ is the pixel surface reflectance.

ρe is an average surface reflectance for the pixel and a surrounding region

S is the spherical albedo of the atmosphere

La is the radiance back scattered by the atmosphere

A and B are coefficients that depend on atmospheric and geometric conditions but not on the surface.

The Spectral bands of single dates were staked on one file for each date for each satellite then, Normalized difference vegetation index (NDVI) was calculated for each single image. This index is a dimensionless one that expresses the presence and density of vegetation, and is calculated according to the following equation

[2]:

$$NDVI = \frac{\rho_{ir} - \rho_r}{\rho_{ir} + \rho_r}$$

where:

ρr and ρir are reflectance values corresponding to red and near-infrared wavelengths respectively. For each date for each satellite. The NDVI time series was stacked on one file for each satellite to study the variability for crop growth stages. Images were mosicked to cover the study area. Delineation of only cultivated lands was carried out. All NDVI images were stacked to produce NDVI multi-temporal image. Maximum and minimum values with variance were calculated from NDVI to identify NDVI threshold value of cultivated areas to isolate cultivated lands. Then, the composite NDVI image was used to create a mask for cultivated areas and isolate these areas from the other land cover types (figure 3).

Maximum likelihood classification was carried out for the different datasets: each single date of Landsat data, each single date of Sintenal-2 data and NDVI composite data. Out of (300) ground check points that were collected during winter season, (200) points were used for classification while (100) points were used for accuracy assessment. Accuracy assessment was performed using Kappa analysis was derived using the formula No (3). This analysis is used to assess classification accuracy from an error matrix. It generates a Kappa coefficient that has a possible range from 0 to 1.

$$K = \frac{N\sum_i^r -1(xi + x + i)}{N^2 - \sum_{i-1}^r (xi + x + i)}$$

There is one possible interpretation of Kappa Coefficient: poor agreement = less than (0.20), fair agreement = (0.20) to (0.40), moderate agreement = (0.40) to (0.60), good agreement = (0.60) to (0.80), very good agreement = (0.80) to (1.00). Flow chart of the whole methodology is explained in figure (2).

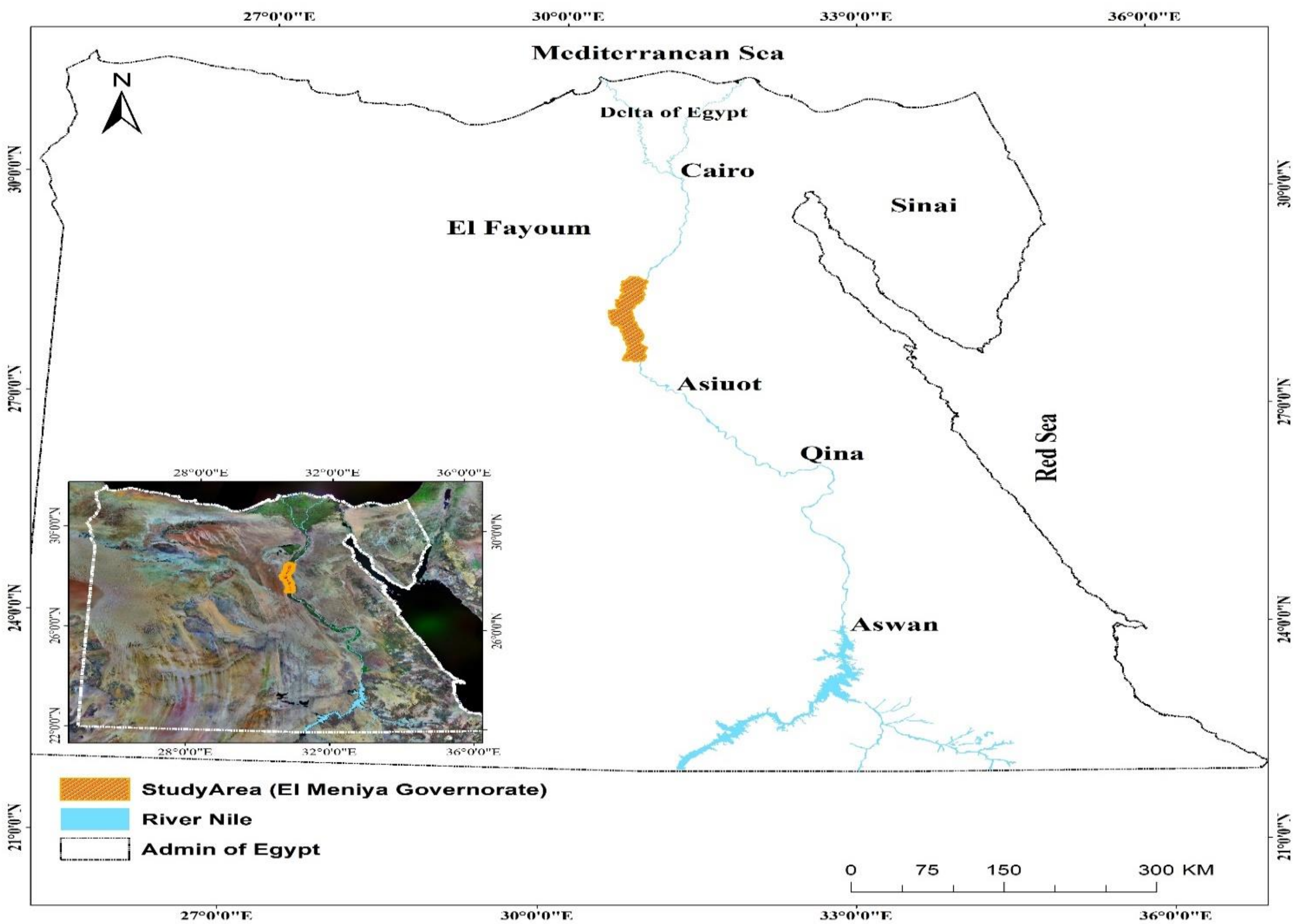

Figure 1. Location of the study area

Table (1): Characteristics of satellite imagery

SentSeinel-2				Landsat-8			
Band Name	Bandwidth (µm)	Resolution (m)	Revisit Time	Band Name	Bandwidth (µm)	Resolution (m)	Revisit Time
Band 2	490nm	10m	10 Days	Band 1 Coastal	0.43 - 0.45	30	16 Days
Band 3	560	10m		Band 2 Blue	0.45 - 0.51	30	
Band 4	665	10m		Band 3 Green	0.53 - 0.59	30	
Band 8	842	10m		Band 4 Red	0.63 - 0.67	30	
Band 5	705	20m		Band 5 NIR	0.85 - 0.88	30	
Band 6	740	20m		Band 6 SWIR 1	1.57 - 1.65	30	
Band 7	783	20m		Band 7 SWIR 2	2.11 - 2.29	30	
Band 8 a	865	20m		Band 8 Pan	0.50 - 0.68	15	
Band 11	1620	20m		Band 9 Cirrus	1.36 - 1.38	30	
Band 12	2190	20m		Band 10 TIRS 1	10.6 - 11.19	30 (100)	
Band 1	443	60m		Band 11 TIRS 2	11.5 - 12.51	30 (100)	
Band9	940	60m					
Band10	1375	60m					

Table 2. Data acquisition

Acquisition Date	**Sensor type**		
Jan/16/2016	**Landsat-8** with(30m) spatial resolution		
Feb/01/2016			
Feb/17/2016			
March/04/2016			
Apr./5/2016			
Apr./21/2016			
Feb/09/2016		**Sentinel-2**with(10m) spatial resolution	**Sentinel-2**with(20m) spatial resolution
Jan/10/2016			
Feb/19/2016			
March/30/2016			
Apr./19/2016			

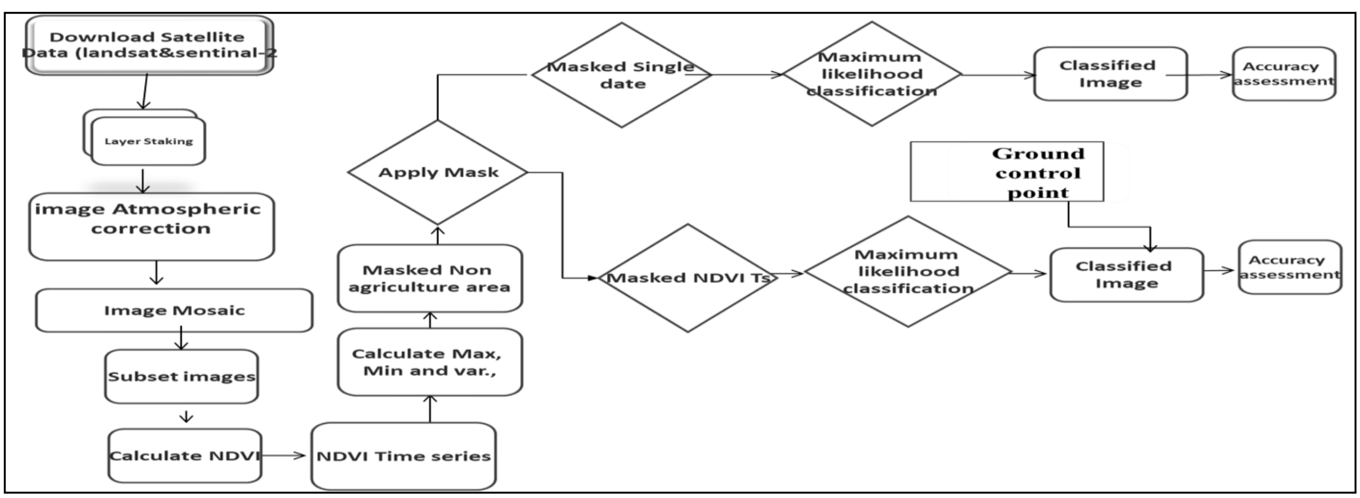

Figure (2) flowchart of methodology

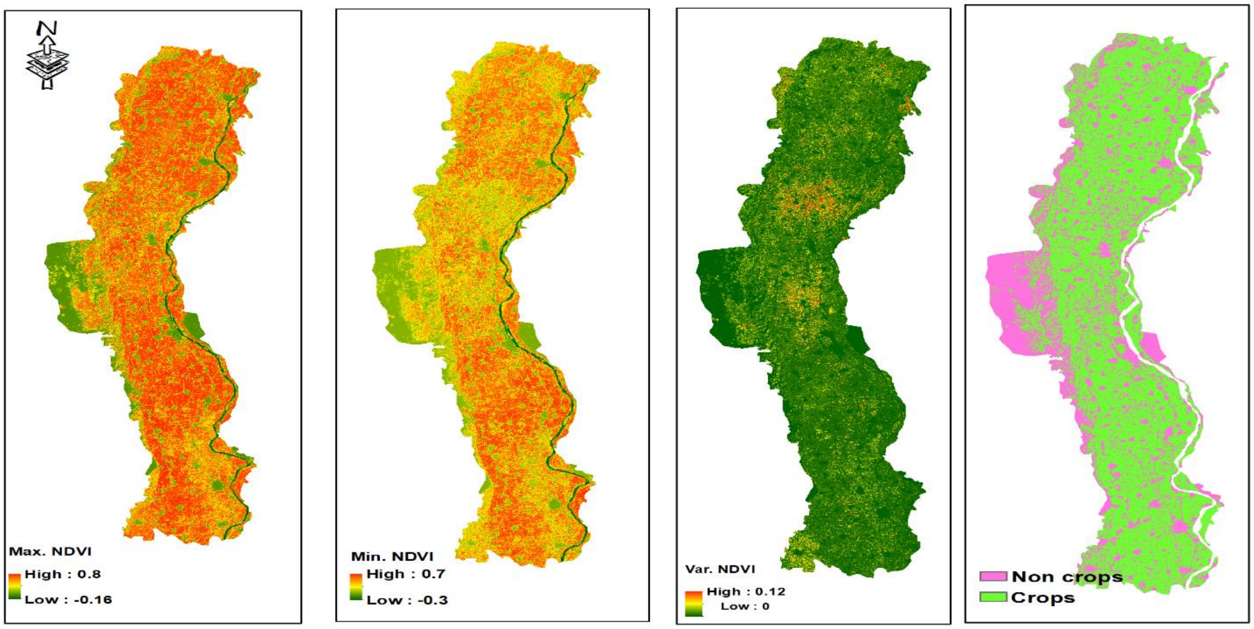

Figure 3. Masking process to isolate cultivated lands

Results and Discussion

Overall accuracy and Kappa coefficients between single date of (Sentinel-2-10m) and times series (NDVI-Ts) generated from Sentinel-2 (10m) as shown in figure (3) indicated that (NDVI Ts) was the optimal dataset with (81%) overall accuracy and (0.74) kappa coefficient. (NDVI Ts) generated from Sentinel-2 (20m) also showed the highest overall accuracy (69.38 %) and highest kappa coefficient (0.58) when compared with single date of Sentinel-2 (20m) as shown in figure

(4). Differently, Landsat-8 data of January 16 showed the highest accuracy comparing with other imagery and better than (NDVI Ts) of landsat-8 data with (76%) overall accuracy and (0.62) kappa coefficient as shown in figure (5).

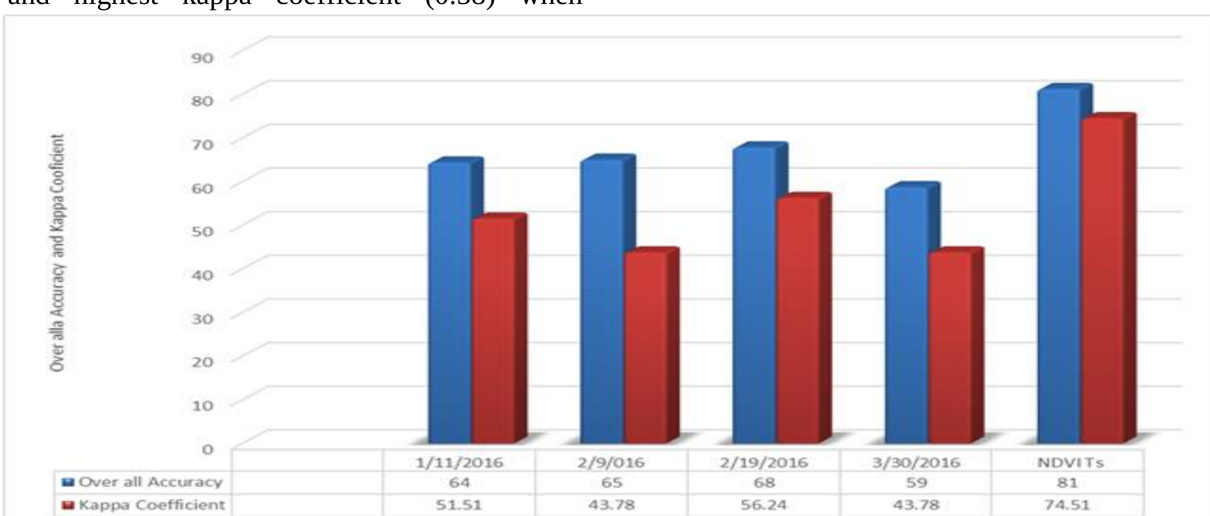

Figure 4. Overall accuracy and Kappa coefficient for Single dates of Sentinel-2 (10m) and the generated NDVI

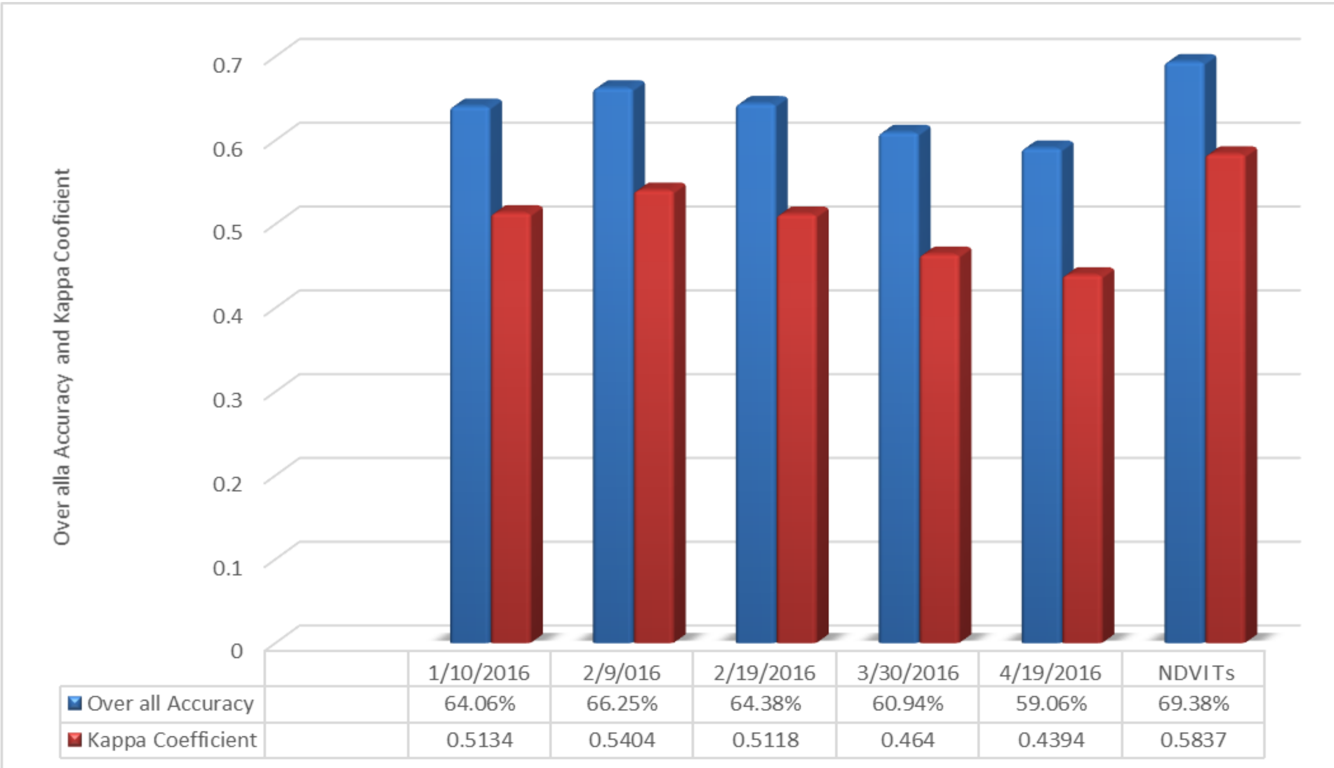

Figure 5. Overall accuracy and Kappa coefficient for Single dates of Sentinel-2 (20m) and the generated NDVI

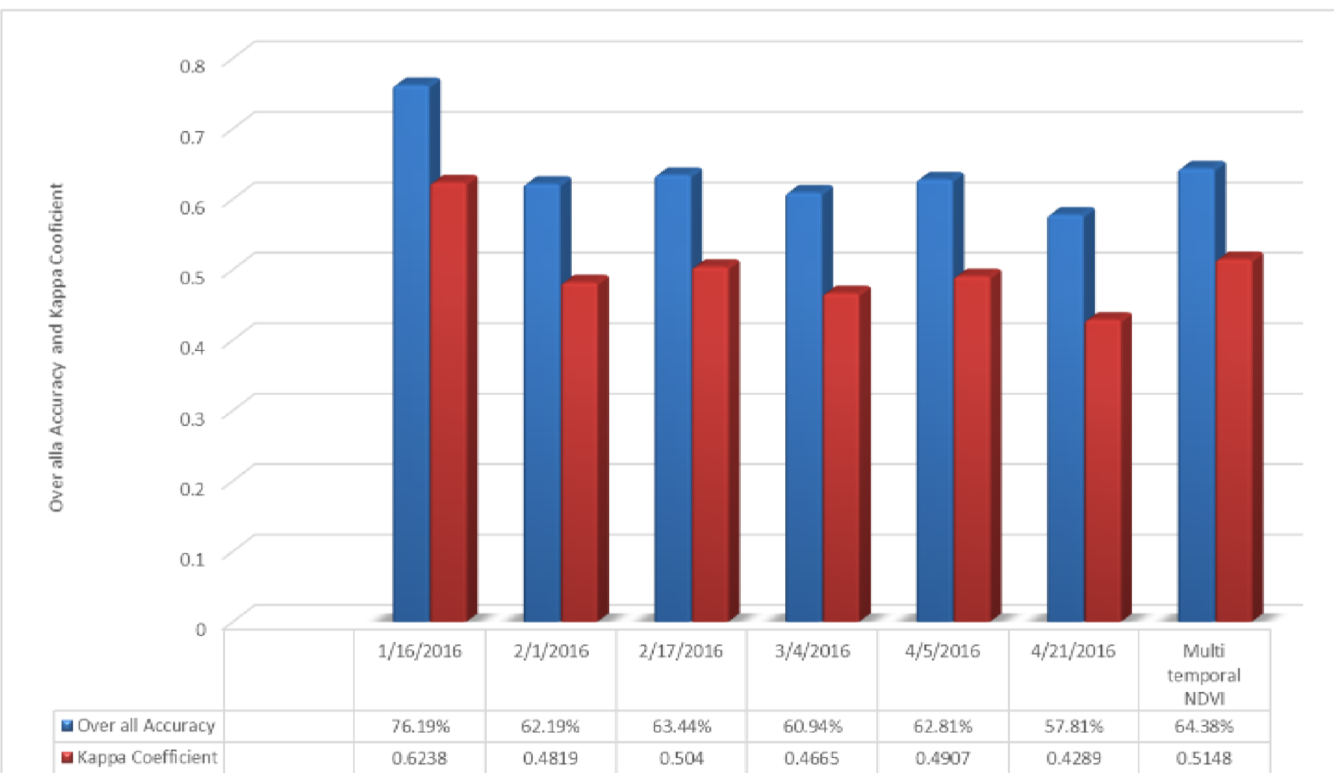

Figure 6. Overall accuracy and Kappa coefficient for Single dates of (Landsat-8) and the generated NDVI

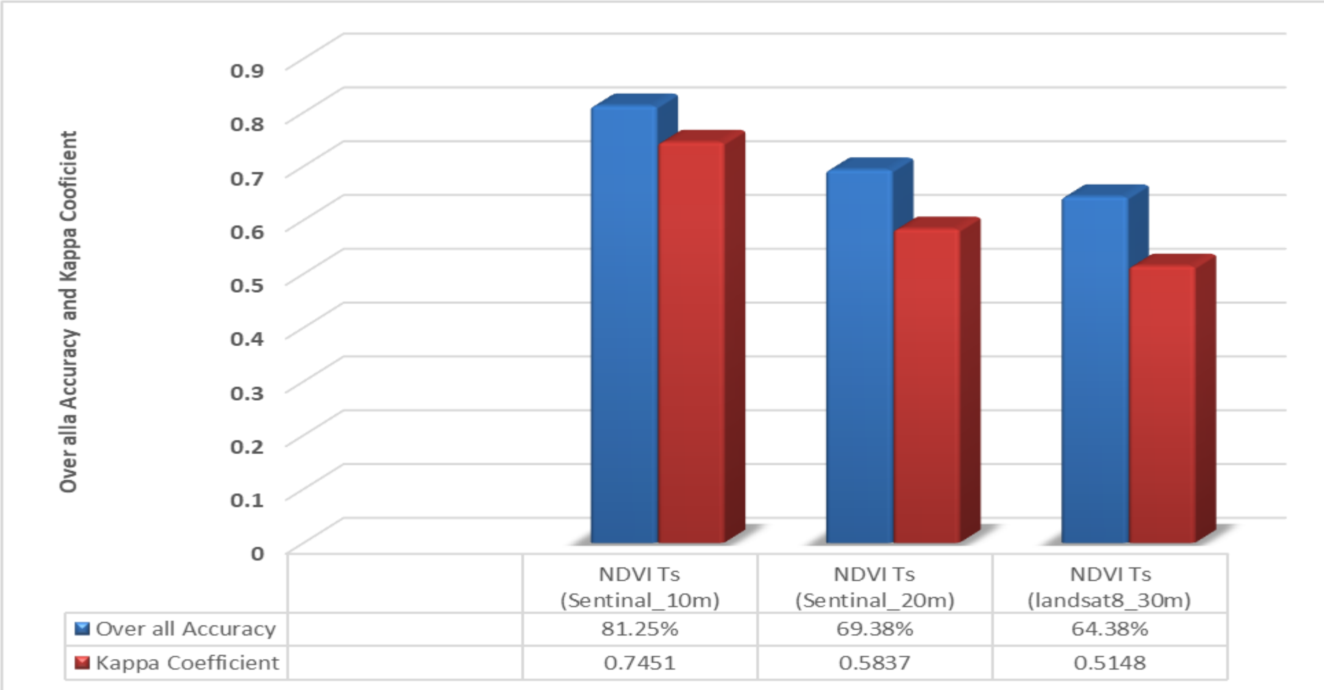

Figure 7. Overall accuracy and Kappa coefficient for NDVI Ts Sentinel-2, (10m and 20m) Landsat-8).

Apart from the overall classification accuracy, which indicates the probability that a given pixel was correctly classified, Table (3) show other measures of the accuracy assessment (producer and user accuracy in NDVITs derived from sentinel-2 with spatial resolution 10 m, NDVI Ts derived from Sentinel -2 with spatial resolution 20 m and NDVI Ts derived from Landsat-8 with spatial resolution 30m respectively). This indicates the level of the accuracy of crop area classes. The producer accuracy was obtained by dividing the number of correctly classified objects by its column total. Producer's accuracy is important as it measures the probability that a reference sample of ground truth data was correctly classified. It is an indication of how accurate a given area in crop area estimation could be mapped.

The lowest value of producer accuracy was (51.72, 64.1, and 32.76) obtained for other crops class and clover NDVITs derived from sentinel-2 20m,10m and NDVITs derived landsat-8) in table (3) respectively. Such a low level of correspondence between classification and reference data is due to the effect of difference between crop growth stages and the different between spatial resolution in the study area and the method of planting and plant distance.

Table (3) Producer and user accuracy for Ts derived from sentinel-2 with spatial resolution 20m, NDVI Ts derived from Sentinel -2 with spatial resolution 10 m and NDVI Ts derived from Landsat-8 with spatial resolution 30m

	Sentinel 20 m Spatial Resolution	**Sentinel 10 m Spatial Resolution**	**Land sat-8 30m Spatial Resolution**			
Class	Prod. Acc. (%)	User Acc.(%)	Prod. Acc. (%)	User Acc.(%)	Prod. Acc. (%)	User Acc.(%)
Clover	53.68	68.92	64.21	85.92	70.53	63.81
Other	51.72	60	75.86	83.02	32.76	55.88
Trees	91.8	69.14	90.16	70.51	86.89	60.92
Wheat	80.19	73.91	94.34	84.75	63.21	71.28

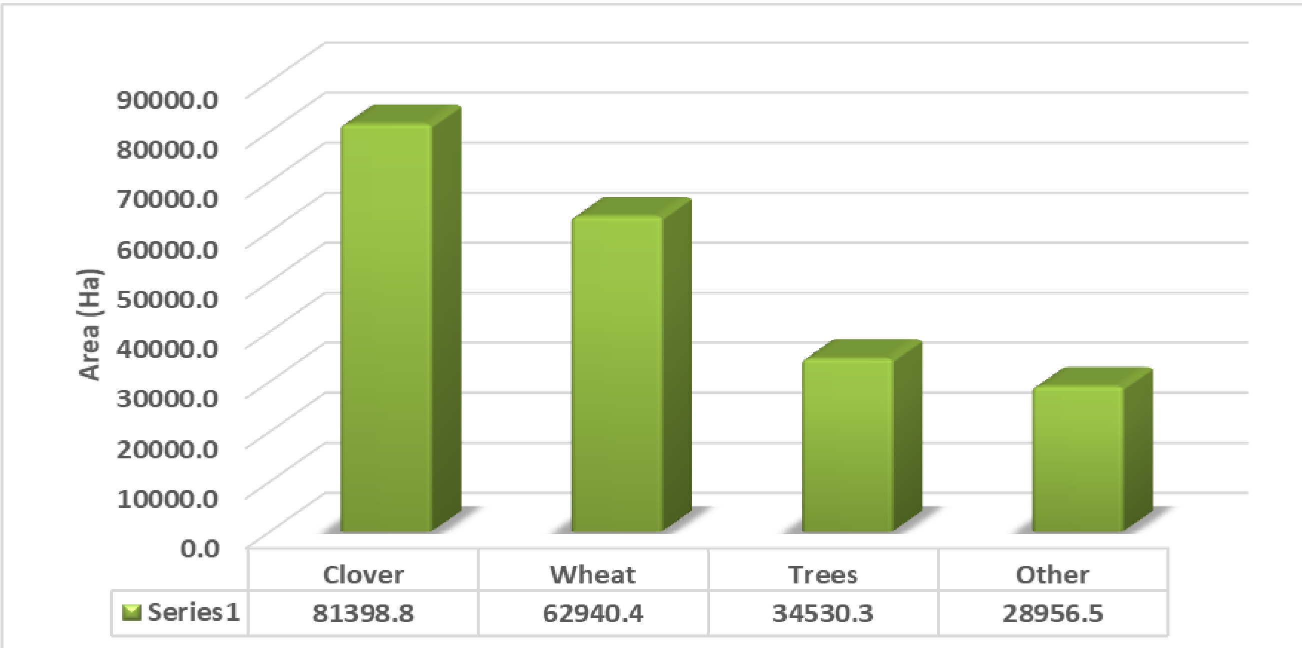

Figure (8):**Total area of the different winter crops in the study area**

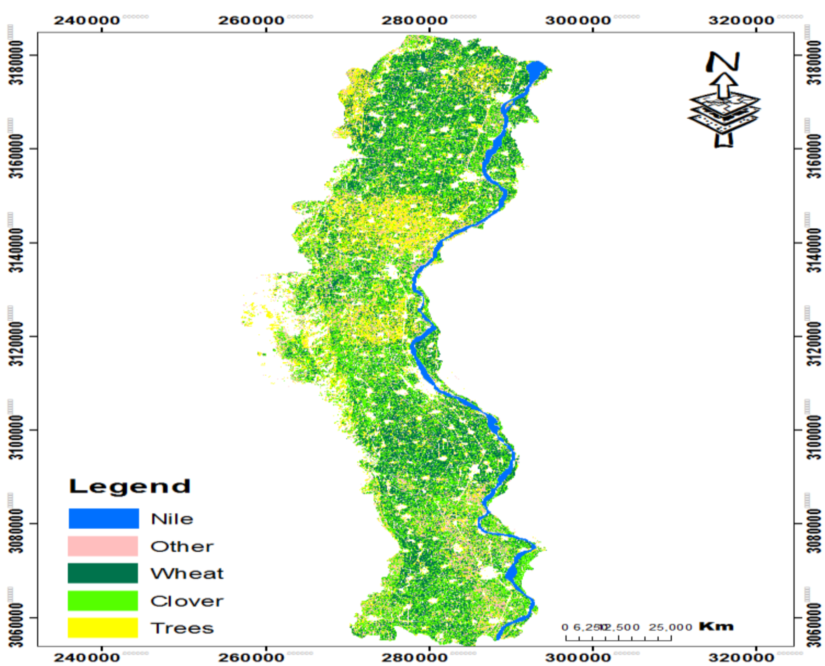

Figure 9. Maximum likelihood classification result of NDVI Ts of Sentinel-2data

The highest value for producer's accuracy was obtained (94.34%) in the (NDVI Ts derived from Sentinel -2 with spatial resolution 10 m) for wheat, comparing with the other classes.
The user's accuracy was obtained by dividing the number of correctly classified objects by its row total. It indicates the probability that an object from the crop area map actually matches ground truth data. The lowest user accuracy values were obtained for other crops class (55%) in NDVITs derived from Landsat-8 with spatial resolution 30 m, Highest user accuracy values were obtained for wheat, trees and clover in

NDVITs derived from Sentinel -2 with spatial resolution 10 m.

It was found that (NDVI Ts of Sentinel-210 m) is the optimal dataset to isolate wheat cultivation in Al-Minya governorate. According to the result of Maximum likelihood classification of Sentinel-2data (figure 8 and 9), the total wheat cultivation area was (62940.4) hectare. Clover occupies the largest crop area (81399) hectare while orchards (mainly Citrus and Grape) cover a total area of (34530) hectare.

Conclusion

Comparative analysis was carried out in order to identify the optimal dataset that could be used ti isolate wheat cultivation in the study area that represents the most agricultural productive governorate in Upper Egypt. The data cover the whole winter season starting from December 2015 to April 2016. Sentinel-2and landsat-8 data were tested to isolate wheat cultivation. Also, using single image was tested versus multi-temporal NDVI for crop classification. The result showed that NDVITs of Sentinel-2data with 10-m spatial resolution was the optimal to isolate wheat crop as explained from overall accuracy and kappa coefficient. Maximum likelihood classifier was then applied on (NDVITs) of (Sentinel-2data 10 m) and the area of the different crops were identified.

References

Drusch M, Del Bello U, Carlier S, Colin O, Fernandez V, Gascon F, Hoersch B, Isola C, Laberinti P, Martimort P, Meygret A, Spoto F, Sy O, Marchese F and Bargellini P, 2010. Sentinel-2: ESA's Optical High-Resolution Mission for GMES Operational Services. Rem. Sens. Environ. 120: 25–36.

Epiphanio R, Dalla V, Formaggio AR, Rudorff BFT, Maeda, EE and Luiz AJB, 2010. Estimating soybean crop areas using spectral‐temporal surfaces derived from MODIS images in Mato Grosso, Brazil. Pesquisa Agropecuária Brasileira, 45: 72‐80.

Food and Agricultural Organization of the United Nations, 2015. Egypt: wheat sector review, pp. 1-88.

Kaufman YJAE, Wald LA, Remer BC, Gao R, Li and Flynn L, 1997. The MODIS 2.1-μ m Channel-Correlation with Visible Reflectance for Use in Remote Sensing of Aerosol. IEEE Transact. Geosci. Rem. Sens. 35: 1286-1298.

Malenovský Z, Rott H, Cihlar J, Schaepman ME, García-Santos G, Fernandes R and Berger M, 2012. Potential of Sentinel-1, -2 and -3 missions for scientific observations of ocean, cryosphere, and land. Rem. Sens. Environ. 120: 91–101.

Manjunath KR, Potdar MB and Purohit, NL, 2002. Large area operational wheat yield model development and validation based on spectral and meteorological data. Int. J. Rem. Sens. 23: 3023–3038.

Pickup G, Chewings VH and Nelason DJ, 1993. Estimating changes in vegetation cover over time in arid rangelands using Landsat MSS data. Rem. Sens. Environ. 43: 243‐263.

Prasad AK, Chai L, Singh RP and Kafatos M, 2006. Crop yield estimation model for Iowa using remote sensing and surface parameters. Int. J. App. Earth Observ. Geoinformat. 8: 26–33.

Ren J, Chen Z, Zhou Q and Tang H, 2008. Regional yield estimation for winter wheat with MODIS‐NDVI data in Shandong, China. Int. J. App. Earth Observ. Geoinformat.10: 403‐413.

Salazar L, Kogan F and Roytman L, 2007. Use of remote sensing data for estimation of winter wheat yield in the United States. Int. J. Rem. Sens. 28: 3795–3811.

Silva GBS, Formaggio DA, Shimabukuro AR, Adami YE and Sano MEE, 2010. Discriminação da coberturavegetaldo erradomatogross ensepormeio deimagens MODIS. Pesquisa Agropecuária Brasileira. 45:186‐194.

Wardlow BD, Kastens J and Egbert SL, 2006. Using USDA crop progress data for the evaluation of green up onset date calculated from MODIS 250‐meter data. Photogram. Engin. Rem. Sens.72: 1225‐1234.